THE ASTROPHYSICAL JOURNAL, 420:1–8, 1994 January 1

COMMENTS ON THE STATISTICAL ANALYSIS OF EXCESS VARIANCE IN THE *COBE*[1] DIFFERENTIAL MICROWAVE RADIOMETER MAPS

E. L. WRIGHT,[2] G. F. SMOOT,[3] A. KOGUT,[4] G. HINSHAW,[4] L. TENORIO,[3] C. LINEWEAVER,[3]
C. L. BENNETT,[5] AND P. M. LUBIN[6]
Received 1993 March 31; accepted 1993 July 12

ABSTRACT

Cosmic anisotropy produces an excess variance σ^2_{sky} in the ΔT maps produced by the Differential Microwave Radiometer (DMR) on *COBE* that is over and above the instrument noise. After smoothing to an effective resolution of 10°, this excess, $\sigma_{sky}(10°)$, provides an estimate for the amplitude of the primordial density perturbation power spectrum with a cosmic uncertainty of only 12%. We employ detailed Monte Carlo techniques to express the amplitude derived from this statistic in terms of the universal rms quadrupole amplitude, $\langle Q^2_{RMS}\rangle^{0.5}$. The effects of monopole and dipole subtraction and the non-Gaussian shape of the DMR beam cause the derived $\langle Q^2_{RMS}\rangle^{0.5}$ to be 5%–10% larger than would be derived using simplified analytic approximations. We also investigate the properties of two other map statistics: the actual quadrupole and the Boughn-Cottingham statistic. Both the $\sigma_{sky}(10°)$ statistic and the Boughn-Cottingham statistic are consistent with the $\langle Q^2_{RMS}\rangle^{0.5} = 17 \pm 5$ μK reported by Smoot et al. (1992) and Wright et al. (1992).

Subject headings: cosmic microwave background — cosmology: observations

1. INTRODUCTION

Smoot et al. (1992) give 30 ± 5 μK for the rms of the cosmic microwave background based on Differential Microwave Radiometer (DMR) maps smoothed to an effective resolution of 10°. This value is derived from the excess variance found using var (sky) = var $[(A + B)/2]$ − var $[(A - B)/2]$, where the $(A + B)/2$ map averages results from the two receivers at each frequency in the DMR instrument, while $(A - B)/2$ is a noise map. These values are computed after the galactic plane region is excised from the map, and a monopole plus dipole fit to the high Galactic latitude sky is subtracted. Because spherical harmonics are no longer orthogonal in the map with the Galactic plane removed, one must modify the usual relationship betewen $\sigma^2_{sky}(10°)$ and the amplitude of the primordial perturbation power spectrum. For power-law density perturbation power spectra of the form $P(k) \propto k^n$, where k is a spatial wavenumber, the rms microwave background anisotropy in the lth order multipoles is

$$\Delta T_l^2 = 0.2(2l+1)\langle Q^2_{RMS}\rangle \frac{\Gamma[l+(n-1)/2]\Gamma[(9-n)/2]}{\Gamma[l+(5-n)/2]\Gamma[(3+n)/2]}, \quad (1)$$

where the normalization is expressed in terms of the universal quadrupole amplitude $\langle Q^2_{RMS}\rangle$ (Bond & Efsthathiou 1987). The analytic formula for the 10° variance, $\sigma_{sky}(10°)$, is then

$$\sigma^2_{sky}(10°) = \sum_{l=2}^{\infty} \Delta T_l^2 \exp\left[-l(l+1)/l_c^2\right], \quad (2)$$

where the smoothing cutoff is $l_c = 180°(8 \ln 2)^{1/2}/(10°\pi) = 13.5$. Equations (1) and (2) were used to compute the conversion factor $\sigma_{sky}(10°)/\langle Q^2_{RMS}\rangle^{0.5} = 2.0 \pm 0.2$ given in Smoot et al. (1992), and an equivalent equation was used by Adams et al. (1993) to convert $\sigma_{sky}(10°)$ into the bias at 8 h^{-1} Mpc^{-1}, b_8. These conversions must be corrected by 5%–10%, however, because the smoothing term in equation (2) does not adequately represent the combined action of the DMR beam and the smoothing techniques used to calculate $\sigma_{sky}(10°)$. The DMR beam is not a perfect Gaussian, and the extra smoothing from the wings of the beam pattern reduces $\sigma_{sky}(10°)$. Furthermore, the monopole plus dipole removal performed on the high Galactic latitude part of the maps also removes part of the quadrupole and octupole which reduces $\sigma_{sky}(10°)$. In this paper we give the filtering effect of the actual DMR beam as a function of multipole order l, a description of two computer programs that have been used to compute $\sigma_{sky}(10°)$, and the results of Monte Carlo calibrations of these programs.

We also use Monte Carlo simulations to compute the expected values of two other quadratic statistics of the DMR maps: the actual Q^2 and the Boughn-Cottingham statistic described by Boughn et al. (1992).

2. DMR BEAM

The beam shape of the DMR horns has been approximated by Smoot et al. (1992) as a Gaussian with a 7° FWHM. this is a reasonable description of the central lobe of the beam, but neglects the sidelobes. Figure 1 shows eight separate traces for the E[7] and H plane measurements of the four 53 GHz flight horns by Toral et al. (1989), the average power response of

[1] The National Aeronautics and Space Administration/Goddard Space Flight Center (NASA/GSFC) is responsible for the design, development, and operation of the *Cosmic Background Explorer* (*COBE*). Scientific guidance is provided by the *COBE* Science Working Group. GSFC is also responsible for the development of the analysis software and for the production of the mission data sets.

[2] UCLA Astronomy Department, Los Angeles CA 90024-1562 (I: wright@astro.ucla.edu).
[3] LBL and SSL, Building 50-351, University of California, Berkeley, Berkeley CA 94720.
[4] Universities Space Research Association, Code 685.3, NASA/GSFC, Greenbelt MD 20771.
[5] NASA/Goddard Space Flight Center, Code 685, Greenbelt MD 20771.
[6] UCSB Physics Department, Santa Barbara CA 93106.

[7] The E plane contains the horn axis and the incident electric field vector.

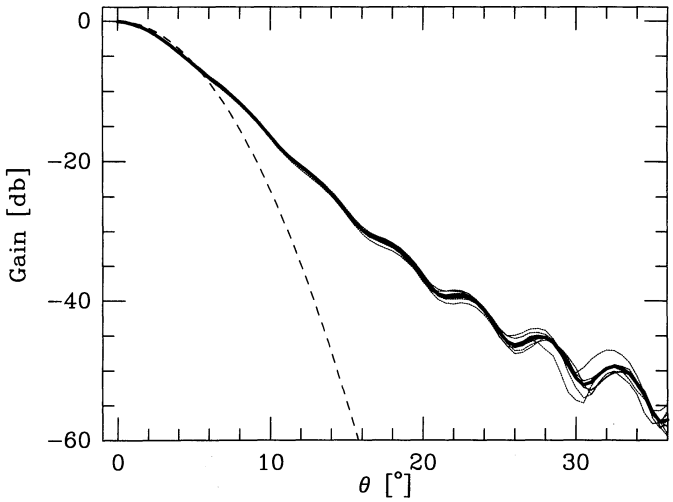

FIG. 1.—The average 53 GHz DMR beam shape (*heavy solid curve*), the eight individual E and H plane traces of the four flight horns (*light dotted lines*), and the Gaussian approximation (*dashed line*).

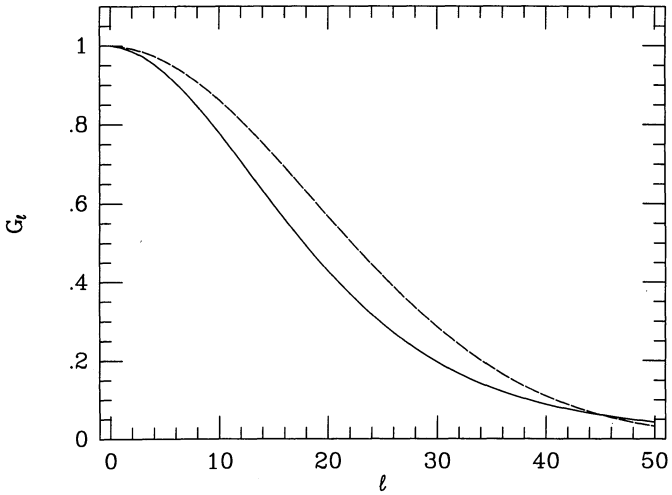

FIG. 2.—The Legendre coefficients of the average DMR beam (*solid*) and of a 7° FWHM Gaussian.

these eight traces as the heavy solid line, and the Gaussian model as a dashed line.

For the purpose of modeling the effect of the DMR beam smoothing on stochastic models described in terms of spherical harmonics, an expansion of the beam profile into Legendre polynomials is needed. We have calculated the coefficients of this expansion for the average of the measured beam profiles using

$$G_l = \int_{-1}^{1} P_l(x) G(\cos^{-1} x) dx \,, \qquad (3)$$

where $G(\theta)$ is the power transmission of the beam (i.e., $G = 0.1$ at 10 db down) and P_l is the lth Legendre polynomial. Since the DMR is calibrated using whole beam signals—hot and cold loads on the ground and Earth velocity signal in space (Bennett et al. 1992a)—we have normalized the G_l's so that $G_0 = 1$. The normalized G_l's are tabulated in Table 1. Figure 2 compares these values to a Gaussian with $\sigma = 2.^{\circ}973$ (FWHM = 7°).

3. SMOOTHING METHODS

Smoothing the DMR maps gives a better estimate of cosmic anisotropy because noise in adjacent pixels is essentially uncorrelated while cosmic signals are expected to have substantial correlations over patches many pixels in size. In a simplified

TABLE 1

RESPONSES AS A FUNCTION OF l NORMALIZED TO 10^4

l	G_l	G_{l+20}	VD20[a,b]	VD30[a,c]	VG20[b,d]	VG30[c,d]	VQ20[b,c]	VS20[b,f]
0	10000	4288	0	0	0	0	0	0
1	9951	3988	0	0	0	0	0	0
2	9855	3703	9354	8483	8920	6659	9989	0
3	9714	3434	8567	6822	7940	4045	26	6342
4	9532	3179	9424	9442	9225	9261	3074	3478
5	9312	2940	9059	9196	8799	8617	10	3776
6	9058	2717	9096	9120	8864	8690	774	2646
7	8774	2508	8804	8778	8508	8141	4	2007
8	8465	2314	8543	8515	8166	8171	74	1441
9	8136	2134	8209	8132	7754	7714	2	1084
10	7791	1967	7856	7849	7340	7340	39	810
11	7435	1813	7473	7474	6882	6850	1	633
12	7072	1671	7094	7096	6450	6491	70	478
13	6705	1540	6686	6687	5987	6032	1	384
14	6338	1420	6291	6288	5550	5590	55	296
15	5975	1310	5879	5871	5102	5124	1	239
16	5617	1209	5475	5473	4669	4716	15	184
17	5268	1117	5070	5068	4245	4293	1	147
18	4929	1033	4673	4671	3840	3891	5	114
19	4602	956	4284	4281	3452	3496	0	90

[a] Statistic: DMRSMUTH.
[b] $b_c = 20°$.
[c] $b_c = 30°$.
[d] Statistic: GET_SKY_RMS.
[e] Statistic: Q^2.
[f] Statistic: S.

case where the cosmic signal is very weak and the observation time per pixel is constant, the uncertainty in var (sky) is given by

$$\text{var [var (sky)]} = \frac{4\sigma^4}{N}, \tag{4}$$

where σ is the noise per pixel in the sum and difference maps (the same in both because the cosmic signal is assumed to be weak), and N is the number of pixels. Smoothing the map by averaging 2 × 2 blocks of pixels reduces σ by a factor of 2 while reducing N by a factor of 4. The net effect is to reduce the standard deviation of var (sky) by a factor of 2. The expected value $\langle \sigma^2_{\rm sky}(10^\circ)\rangle$ is reduced by a much smaller factor for cosmic models with substantial large-scale power, such as the Harrison-Zel'dovich spectrum with equal power on all scales. Thus smoothing the DMR maps with a smoothing kernel having the same width as the DMR beam gives a useful estimate of the cosmic anisotropy. Two distinct smoothing techniques have been developed to smooth the DMR maps and estimate $\sigma_{\rm sky}(10^\circ)$. The computer programs that implement these algorithms, called GET_SKY_RMS and DMRSMUTH, are available by E-mail from the first author.

3.1. *Unweighted Smoothing*

DMRSMUTH is the program used by Wright (1991) to estimate an excess variance of 1024 ± 450 μK^2 for $|b| > 15^\circ$ in the 6 month 53 GHz maps (Smoot et al. 1991). This value is in Rayleigh-Jeans temperature differences $\Delta T_{\rm RJ}$, related to the desired Planck temperature differences $\Delta T_{\rm P}$ by

$$\Delta T_{\rm RJ} = \frac{x^2 e^x}{(e^x - 1)^2}\,\Delta T_{\rm P} \tag{5}$$

with $x = h\nu/kT$. The DMRSMUTH program smooths a map using a quasi-Gaussian test function which has continuous derivatives of all orders and is nonzero only in a small region, thereby reducing the number of computations. To be precise, the function is

$$S(\theta) = \exp\left\{-8\ln 2\left[\frac{1}{1 - \sin^2(\theta/2)/\sin^2(\theta_c/2)} - 1\right]\right\} \tag{6}$$

with $\theta_c = 10.^\circ5$. The FWHM of this function is $7.^\circ0$, but it vanishes smoothly for all angles $> 10.^\circ5$. For a given input map, t_i, the smoothed output map T_j is given by

$$T_j = \frac{\sum_i t_i S(\theta_{ij})}{\sum_i S(\theta_{ij})}, \tag{7}$$

where θ_{ij} is the distance between the ith and jth pixels. All sums are done over a grid of 24,576 pixels. Since the DMR maps have 6,144 pixels, each DMR pixel is copied into the 4 pixels in a 2 × 2 block of pixels. After the entire sky is smoothed, the Galactic plane with $|b| < b_c$ is discarded and a monopole plus dipole is fitted and removed from the polar caps. The unweighted variance of the residuals in the polar caps is the result.

3.2. *Weighted Smoothing*

The second program, GET_SKY_RMS, was used by Smoot et al. (1992) to compute $\sigma_{\rm sky}(10^\circ) = 41$, 30, 30, and 30 μK in thermodynamic ΔT for the 1 yr 53 GHz maps with Galactic plane cuts of 10°, 20°, 30°, and 40°. GET_SKY_RMS differs from DMRSMUTH in several significant respects. The first difference is the smoothing kernel: GET_SKY_RMS uses an exact Gaussian with a σ of $3.^\circ000$, so its FWHM is $7.^\circ064$. GET_SKY_RMS does its sums on the DMR 6144 pixel grid. The second major difference is that GET_SKY_RMS uses weighted sums in its smoothing. Let $R(\theta)$ be the Gaussian smoothing kernel. Then the smoothed map from GET_SKY_RMS is

$$T_j = \sum [t_i w_i R(\theta_{ij})] / \sum [w_i R(\theta_{ij})]\,. \tag{8}$$

The input weights w_i used above are set to zero in the region $|b| < b_c$ before the smoothing is done. Thus for a new value of b_c, the map must be resmoothed, while for DMRSMUTH all values of b_c use the same smoothed map. The weights W_j for the smoothed map are computed using the normal propagation of error technique:

$$W_j = \{\sum [w_i R(\theta_{ij})]\}^2 / \sum [w_i R(\theta_{ij})^2]\,. \tag{9}$$

A monopole plus dipole fit is removed twice: once before smoothing using the weights w_i, and then again to T_j after smoothing using the weights W_j. Because the weights in $|b| < b_c$ are set to zero before the smoothing, the pixels at edge of the polar caps have only half the weight of pixels in the middle. Furthermore, the centroid of the weight contributing to an edge pixel is a few degrees away from the edge due to the absence of pixels across the boundary. When compared to DMRSMUTH with the same value for b_c, the effective Galactic plane cutoff is a few degrees higher for GET_SKY_RMS. Finally, the variance computed by GET_SKY_RMS also uses the weights W_j.

3.3. *Response to Multipoles*

Neither program knows the correct values of a_{00} or a_{lm}. Thus when fitting for the monopole and dipole to remove from the maps, both programs make a least-squares fit in the part of the sky with $|b| > b_c$. In this region, the monopole is *not* orthogonal to the quadrupole, and the dipole is *not* orthogonal to the octupole. Thus the monopole plus dipole fit removes a significant part of the quadrupole and octupole as well. In order to quantify this effect, all of the spherical harmonics with $l < 20$ were processed by each smoothing technique one at a time. Let V_{lm} be the variance given by the spherical harmonic F_{lm}, where we use real spherical harmonics normalized to unit variance over the whole sky.[8] Thus for $b_c = 0$ and no smoothing we have $V_{lm} = 1$ for all l and m. Given the smoothing and $b_c > 0$, some of the V_{lm}'s are very small while others are larger than 1. The quantity required to estimate the average responses of DMRSMUTH and GET_SKY_RMS to a cosmological model is the mean of V_{lm} over m:

$$V_l = \frac{\sum V_{lm}}{2l + 1}\,. \tag{10}$$

Figure 3 shows this net filter function for the two programs and for $b_c = 20^\circ$ and 30°. In Table 1 the columns labeled VD20

[8] These F_{lm}'s are $(4\pi)^{1/2}$ times the functions defined in Smoot et al. (1991), but note the typo: $(1 - m)!$ should be $(l - m)!$

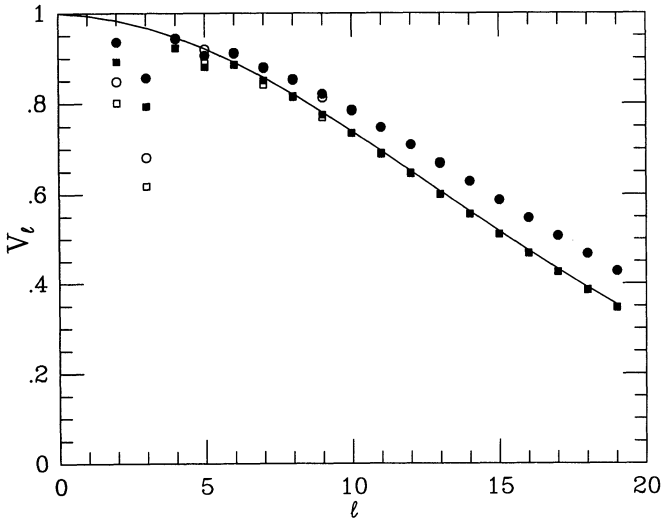

FIG. 3.—The average variance in the smoothed, dipole-removed map for unit input variance in order l. Circles are DMRSMUTH and squares are GET_SKY_RMS, filled symbols are $b_c = 20$, and open symbols are $b_c = 30°$. The solid line shows the analytic formula for a Gaussian smoothing kernel with $\sigma = 3°$ and $b_c = 0$.

and VD30 give V_l for DMRSMUTH with 20° and 30° cuts, while VG20 and VG30 gives the values for GET_SKY_RMS.

With the appropriate smoothing functions for the beam G_l and the response of the smoothing techniques V_l, we can revise equation (2) to read

$$\sigma^2_{\rm sky}(10°) = \sum_{l=2}^{\infty} \Delta T_l^2 \, G_l^2 \, V_l \, . \tag{11}$$

The ratio of $\langle \sigma^2_{\rm sky}(10°)\rangle / \langle Q^2_{\rm RMS}\rangle$ as a function of the spectral index n is shown in Figure 4. We have approximated V_l for $l > 19$ and G_l for $l > 39$ using Gaussians that match the last

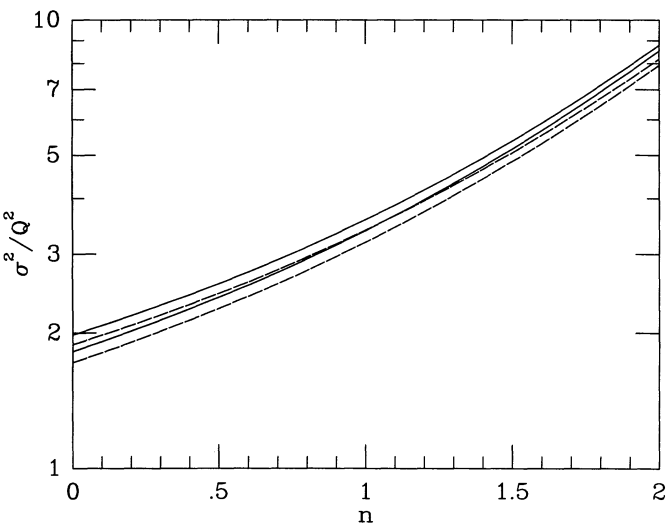

FIG. 4.—The ratio of the excess variance of the smoothed sky to the quadrupole normalized power spectrum amplitude as a function of spectral index of the power spectrum. The solid curves are for DMRSMUTH, while the dashed curves are for GET_SKY_RMS. In each case, the upper curve has $b_c = 20°$ and the lower curve has $b_c = 30°$. The dotted curve shows the relation for a 10° Gaussian beam with $b_c = 0$ computed using eq. (1).

tabulated value when evaluating equation (11). From the slope of the curves in Figure 4 we can estimate an effective angular scale for the $\sigma_{\rm sky}(10°)$ statistic,

$$l_{\rm eff} = 2 \exp \left[\left. \frac{\partial \ln (\sigma^2/Q^2)}{\partial n} \right|_{n=1} \right] . \tag{12}$$

Note that $l_{\rm eff}$ depends on the slope of the input spectrum, and we have used an $n = 1$ slope. The values of $l_{\rm eff}$ are 4.16 and 4.29 for DMRSMUTH with 20° and 30° galaxy cuts, compared to 4.12 and 4.26 for GET_SKY_RMS.

3.4. *Monte Carlo Results*

Monte Carlo skies are generated for power-law density perturbation power spectra, $P(k) = Ak^n$. In order to simulate the effect of the binning within a pixel, the Monte Carlo skies are generated on a grid of 24,576 pixels and then averaged in 2 × 2 blocks to give the standard DMR map with 6144 pixels.

The first step in producing a random map is to generate the $(l_{\rm max} + 1)^2$ random amplitudes a_{lm}. These are generated using a Gaussian random number function with zero mean and a variance given by

$$\text{var}\,(a_{lm}) = 0.2 \, \frac{\Gamma[l + (n-1)/2]\Gamma[(9-n)/2]}{\Gamma[l + (5-n)/2]\Gamma[(3+n)/2]} \, . \tag{13}$$

These values can be generated by setting var $(a_{2m}) = 0.2$ and then using

$$\text{var}\,(a_{l+1,\,m}) = \frac{\text{var}\,(a_{lm})(2l + n - 1)}{(2l - n + 5)} \, . \tag{14}$$

The random sky is then generated using a set of real spherical harmonics F_{lm} that are normalized to have an rms value of unity. With these functions, the sky is given by

$$T(\theta, \phi) = \langle Q^2_{\rm RMS}\rangle^{0.5} \sum_{lm} G_l \, a_{lm} \, F_{lm}(\theta, \phi) \, . \tag{15}$$

The smoothing caused by motion of the DMR beam during the 0.5 s sampling interval has not been included in these Monte Carlo maps. The DMR scans 180° in the *COBE* spin period of ≈73 s, so this produces a boxcar smoothing with width 1°.23 in the scan direction. Since most pixels are observed with scan directions distributed fairly uniformly, this smoothing can be approximated by a circular Gaussian smoothing with $\sigma = 1°.23/(2 \times 12)^{1/2} = 0°.25$, which has a negligible effect (<0.1% in $\langle Q^2_{\rm RMS}\rangle^{0.5}$ for $n < 2$) on the statistics considered in this paper.

We have constructed Monte Carlo skies using the formula given in equation (15) with $l_{\rm max} = 39$. For each Monte Carlo sky, we make two independent noise maps, for the A and B channels of the DMR. We construct these noise maps using the number of observations of each pixel $N_{\rm obs}(i)$ in the actual DMR data maps. Thus each pixel i has an initial noise estimate n_i given by a Gaussian random variable with zero mean and variance given by $\sigma_1^2/N_{\rm obs}(i)$, where σ_1 is the noise per observation of the DMR. We then make a small correction to these noise maps to allow for the fact that the pixels within the map are not perfectly independent. We take the sparse correlation matrix A_{ij}, which has diagonal elements equal to $N_{\rm obs}$ and off-diagonal elements that are the negative of the number of times a given pixel-pair (i, j) was observed. The corrected noise

TABLE 2

MEAN AND STANDARD DEVIATIONS OF $\sigma^2_{sky}(10°)$, S AND Q^2 FROM MONTE CARLO CALCULATIONS COMPARED TO OBSERVED VALUES FROM THE 1 YEAR 53 GHz MAPS, IN PLANCK ΔT μK

MODEL		DMRSMUTH		GET_SKY_RMS		B-C S	Q^2
$\langle Q^2_{RMS}\rangle^{0.5}$ (μK)	Noise	$\lvert b\rvert > 20°$ (μK^2)	$\lvert b\rvert > 30°$ (μK^2)	$\lvert b\rvert > 20°$ (μK^2)	$\lvert b\rvert > 30°$ (μK^2)	$\lvert b\rvert > 20°$ (μK^2)	$\lvert b\rvert > 20°$ (μK^2)
0	Y	0 ± 147	0 ± 168	0 ± 121	0 ± 137	0 ± 24	0 ± 25
13.60	Y	663 ± 237	628 ± 260	633 ± 222	594 ± 240	176 ± 79	216 ± 153
16.66	Y	996 ± 303	941 ± 326	948 ± 290	891 ± 309	264 ± 110	324 ± 219
19.23	Y	1328 ± 373	1255 ± 397	1264 ± 360	1187 ± 381	351 ± 141	431 ± 286
16.66	N	997 ± 229	942 ± 237	944 ± 224	886 ± 231	262 ± 94	322 ± 200
16.66	Y-N	-1 ± 198	-1 ± 228	4 ± 175	5 ± 197	2 ± 54	2 ± 91
Observed.....		1200	1066	924	934	298	107

map is then given by

$$n_i \leftarrow n_i - \sum_{j \neq i} A_{ij} n_j / A_{ii} , \tag{16}$$

which is a first approximation to the inversion of A that is done in the map-making process. The net effect of this correction is to add the weighted mean of all the pixels in the 60° radius reference ring to the value of the ith pixel. This correction has an insignificant effect on $\sigma_{sky}(10°)$ but does increase the noise at $l = 6$ in the DMR power spectrum calculation of Wright (1993). It also creates a small positive correlation at a separation of $60° \pm 5°$ in the autocorrelation function given in Wright et al. (1992) that is not present in the cross-correlation function in Smoot et al. (1992).

Five different combinations of $\langle Q^2_{RMS}\rangle^{0.5}$ and noise level have been simulated for each smoothing technique. These have $\langle Q^2_{RMS}\rangle^{0.5} = 0$, 13.6, 16.66, and 19.23 μK (Planck), with the noise level corresponding to the 1 yr 53 GHz maps, and $\langle Q^2_{RMS}\rangle^{0.5} = 16.66$ μK repeated with no noise. For each of these five cases, the same random noise and Harrison-Zel'dovich maps are smoothed, and then combined with appropriate coefficients before evaluating $\sigma^2_{sky}(10°)$. For a given Monte Carlo realization, $\sigma^2_{sky}(10°)$ is a quadratic polynomial in $\langle Q^2_{RMS}\rangle^{0.5}$, so results for amplitudes other than the ones calculated can be obtained by interpolation. The mean and standard deviation of $\sigma^2_{sky}(10°)$ and other quadratic statistics from these Monte Carlo realizations are tabulated in Table 2. All of these results are Planck ΔT's, and the maps have been corrected for the kinematic quadrupole due to the second-order Doppler shift, using the observed dipole to define our velocity relative to the cosmic standard of rest (Fixsen et al. 1994; Kogut et al. 1993). From these values we learn several important results.

First, the mean values from the Monte Carlo realizations agree with values calculated from equation (11) with errors that are smaller than the 0.5% uncertainty in the Monte Carlo means. In the $n = 1$ case these ratios are for DMRSMUTH with $\lvert b\rvert > 20°$, $\langle \sigma^2_{sky}(10°)\rangle / \langle Q^2_{RMS}\rangle = 3.584 = 1.892^2$ from equation (11) versus 3.594 ± 0.017 from the Monte Carlo realizations; with $\lvert b\rvert > 30°$, $3.388 = 1.841^2$ versus 3.394 ± 0.017; for GET_SKY_RMS with $\lvert b\rvert > 20°$, $3.395 = 1.843^2$ versus 3.403 ± 0.016; and with $\lvert b\rvert > 30°$, $3.191 = 1.786^2$ versus 3.195 ± 0.017.

Second, the uncertainties in cases done without noise allow us to calculate the ultimate power of these statistics for estimating $\langle Q^2_{RMS}\rangle^{0.5}$ when the integration time is much longer than 1 yr. Equation (11) *cannot* be used to estimate the uncertainty in $\sigma^2_{sky}(10°)$. The ultimate accuracy of an estimate of $\langle Q^2_{RMS}\rangle^{0.5}$ based on $\sigma_{sky}(10°)$ from DMRSMUTH with $\lvert b\rvert > 30°$ will be a relative uncertainty on $\langle Q^2_{RMS}\rangle^{0.5}$ of $0.5 \times 237/942 = 12.6\%$, while from GET_SKY_RMS with $\lvert b\rvert > 20°$ it will be $0.5 \times 224/944 = 11.9\%$.

Third, the uncertainties in the cases with noise can be used to calculate the statistical uncertainty in $\langle Q^2_{RMS}\rangle^{0.5}$ estimated from the current data set. To avoid double counting the experimental uncertainty, no errors should be attached to the observed values, since the noise is already included in the Monte Carlo models. It is difficult to isolate a purely observational error since the effect of radiometer noise on $\sigma^2_{sky}(10°)$ depends on the true pattern of anisotropy $\Delta T(l, b)$ which is not yet known. The differences between $\sigma^2_{sky}(10°)$ computed with noise and $\sigma^2_{sky}(10°)$ without noise for $\langle Q^2_{RMS}\rangle^{0.5} = 16.66$ μK are given in the row labeled "Y-N" in the "Noise" column of Table 2, and these represent the effect of radiometer noise on a typical Harrison-Zel'dovich sky with $\langle Q^2_{RMS}\rangle^{0.5} = 16.66$ μK. The standard deviations shown in this row are much bigger than those in the $\langle Q^2_{RMS}\rangle^{0.5} = 0$ case, showing that the effect of radiometer noise depends on $\langle Q^2_{RMS}\rangle^{0.5}$. Clearly the effect of noise will also depend on n. The current accuracy of an estimate of $\langle Q^2_{RMS}\rangle^{0.5}$ based on $\sigma_{sky}(10°)$ from DMRSMUTH with $\lvert b\rvert > 30°$ is a relative uncertainty on $\langle Q^2_{RMS}\rangle^{0.5}$ of $0.5 \times 326/941 = 17.3\%$, while from GET_SKY_RMS with $\lvert b\rvert > 20°$ it is $0.5 \times 290/948 = 15.3\%$.

In Figures 5 and 6 we have plotted the cumulative probability distribution of these Monte Carlo calculations after converting the probability into a number of "sigma" by inverting the Gaussian cumulative probability function,

$$P(x) = \frac{1}{\sqrt{2\pi}} \int_{-\infty}^{x} \exp\left(\frac{-y^2}{2}\right) dy \tag{17}$$

which is the probability that a zero mean, unit variance Gaussian random variable will be $< x$. A straight line on these plots indicates a normally distributed random variable. The slope of the line is the inverse of the standard deviation, so the reduced slope of the $\langle Q^2_{RMS}\rangle^{0.5} > 0$ cases compared to the $\langle Q^2_{RMS}\rangle^{0.5} = 0$ case shows the effect of cosmic variance. The curvature of the lines, with slope decreasing as $\sigma^2_{sky}(10°)$ increases, indicates a positive skewness in the distribution of $\sigma^2_{sky}(10°)$. An interesting point to note is that the observed excess variance of the sky deviates from the blank sky case by more than 6 σ, even though we have only a 3 σ determination of $\langle Q^2_{RMS}\rangle$.

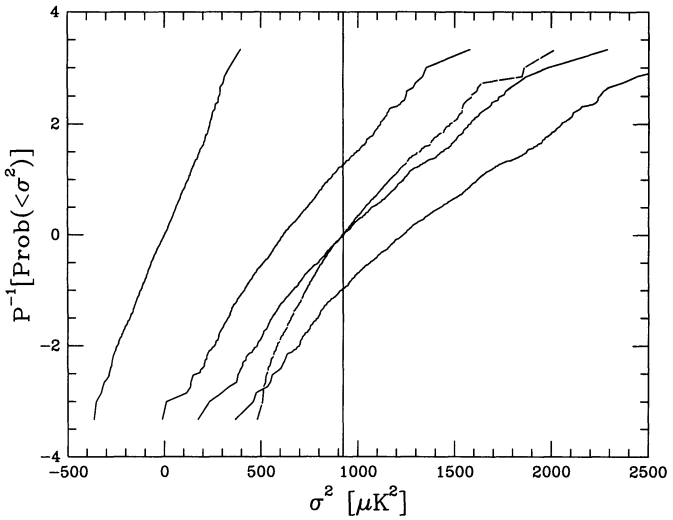

FIG. 5.—The distribution of excess variances determined by GET_SKY_RMS in $|b| > 20°$ for Monte Carlo skies with spectral index $n = 1$, $\langle Q_{\rm RMS}^2\rangle^{0.5} = 0$, 13.6, 16.7, and 19.2 μK with the 1 yr noise, and $\langle Q_{\rm RMS}^2\rangle^{0.5} = 16.7$ μK with no noise (*dashed*). The y-axis is the cumulative probability distribution function from the Monte Carlo's converted into a number of "sigma" by inverting the Gaussian probability distribution function $P(y)$, the probability that a zero mean, unit variance Gaussian random variate will be less than y. The vertical line is the observed value.

4. BOUGHN-COTTINGHAM STATISTIC

The Boughn-Cottingham statistic (Boughn et al. 1992) is a weighted least-squares fit of a line to the cross-products of pixel pairs, based on an expected pattern of correlation for a given model. We write it as

$$S = \frac{(\sum_{ij} w_i\, w_j\, C_{ij}\, t_i^A t_j^B)}{(\sum_{ij} w_i\, w_j\, C_{ij}^2)}\,, \qquad (18)$$

where the coefficient matrix C_{ij} is the expected correlation between the ith and jth pixels for a model with $n = 1$ and $\langle Q_{\rm RMS}^2\rangle^{0.5} = 1$. With normalization given above the expected value of $S = \langle Q_{\rm RMS}^2\rangle$. In order to reduce the size of the matrices involved we have first summed the DMR maps into 2×2 blocks of pixels. We hae evaluated C_{ij} using the 20,000 Monte Carlo skies after removing the monopole dipole, and quadrupole from the part of the sky with $|b| > 20°$. Because of the Galactic plane cut, C_{ij} is a function not only of the separation angle between the ith and jth pixels, but also depends on the latitudes of the pixels as well. The Monte Carlo skies used to construct C_{ij} were generated using a Gaussian approximation for the DMR beam which gives a slightly different value for C_{ij} than a calculation with the DMR beam given by G_l. As a result, we do not assume that $\langle Q_{\rm RMS}^2\rangle^{0.5} = S^{1/2}$ but instead calibrate the Boughn-Cottingham statistic using the same Monte Carlo technique used to calibrate $\sigma_{\rm sky}(10°)$. For the C_{ij} that we use, the expected vaue of S is $\langle S\rangle = (0.943 \pm 0.007)\langle Q_{\rm RMS}^2\rangle$ where the uncertainty is based on 2499 Monte Carlo skies. The actual value of the Boughn-Cottingham statistic for the first year 53 GHz maps is $S = 298$ μK^2 (Planck).

Since there are 6144 pixels in DMR maps, there are 37,748,736 coefficients in C_{ij}. By adjusting the coefficient array, one can create all possible quadratic statistics using equation (18). These include $\sigma_{\rm sky}^2(10°)$, $Q_{\rm RMS}^2$, and every bin of the correlation function $C(\theta)$. The Boughn-Cottingham choice of C_{ij} equal to the expected correlation for the cosmic model is the most efficient choice (gives the lowest uncertainty in $\langle Q_{\rm RMS}^2\rangle^{0.5}$) but only in the limit of weak correlations. This efficiency for weak correlations is shown in Figure 7, where the extrapolation of the $\langle Q_{\rm RMS}^2\rangle^{0.5} = 0$ line crosses the observed value at >12 σ. However, the effect of cosmic variance is larger on S than on $\sigma_{\rm sky}^2(10°)$. Using S to determine $\langle Q_{\rm RMS}^2\rangle^{0.5}$ gives an accuracy of 21%, while using $\sigma_{\rm sky}(10°)$ from DMRSMUTH with $|b| > 30°$ gives an accuracy of 17% from the Monte Carlo skies with the actual noise and an assumed $\langle Q_{\rm RMS}^2\rangle^{0.5} = 16.66$ μK. The value of $\langle Q_{\rm RMS}^2\rangle^{0.5}$ in the Monte Carlo skies necessary to give the expected value of S equal to the observed value is 17.8 μK.

The response of the Boughn-Cottingham statistic, S, to unit rms real spherical harmonics F_{lm}, averaged over m, is given in

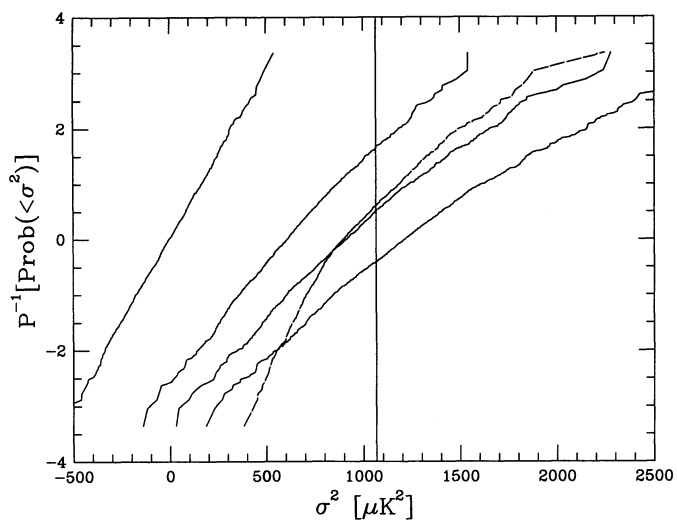

FIG. 6.—The distribution of excess variances determined by DMRSMUTH in $|b| > 30°$ for Monte Carlo skies with spectral index $n = 1$, $\langle Q_{\rm RMS}^2\rangle^{0.5} = 0$, 13.6, 16.7, and 19.2 μK with the 1 yr noise, and $\langle Q_{\rm RMS}^2\rangle^{0.5} = 16.7$ μK with no noise (*dashed*). The vertical line is the observed value.

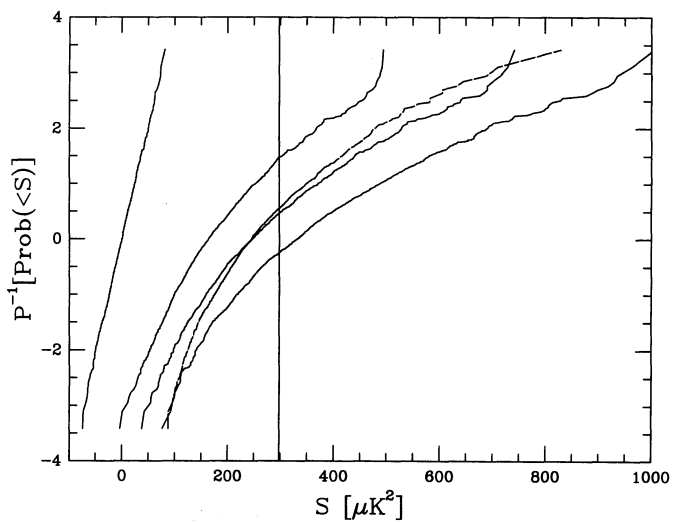

FIG. 7.—The distribution of Boughn-Cottingham statistic $S = |b| > 20°$ for $n = 1$ maps with $\langle Q_{\rm RMS}^2\rangle^{0.5} = 0$, 13.6, 16.7, and 19.2 μK with the 1 yr noise, and for $\langle Q_{\rm RMS}^2\rangle^{0.5} = 16.7$ μK with no noise. The monopole, dipole, and quadrupole found in $|b| > 20°$ are removed from the maps before computing S. The vertical line is the observed value.

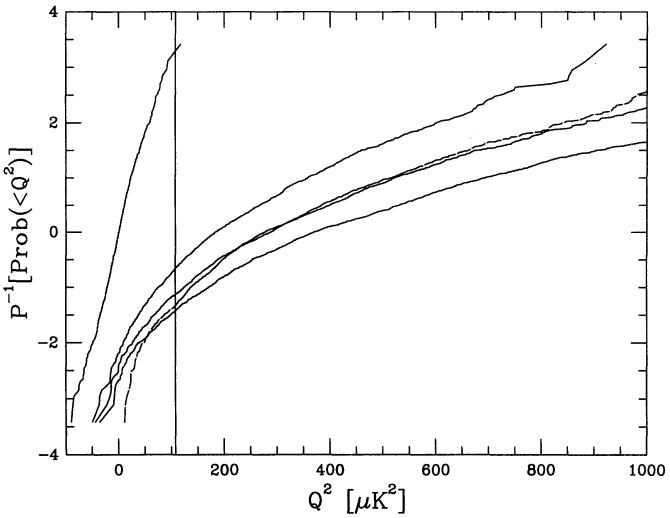

FIG. 8.—The distribution of the actual $Q^2_{\rm RMS}$ in $|b| > 20°$ for $n = 1$ maps with $\langle Q^2_{\rm RMS}\rangle^{0.5} = 0$, 13.6, 16.7, and 19.2 μK with the 1 yr noise, and for $\langle Q^2_{\rm RMS}\rangle^{0.5} = 16.7$ μK with no noise. The vertical line is the observed value.

column VS20 of Table 1. Summing this column times $G_l^2 \Delta T_l^2$ for $n = 1$ also gives $\langle S\rangle = 0.943 \times \langle Q^2_{\rm RMS}\rangle$, and applying equation (12) to the sum for other values of n gives $l_{\rm eff} = 3.96$.

5. ACTUAL QUADRUPOLE

The final example of a quadratic statistic that we consider is the actual $Q^2_{\rm RMS}$ of the map. The statistic calculated from a given location within the universe and with a given b_c should not be confused with the amplitude $\langle Q^2_{\rm RMS}\rangle$, which is the average over the universe of $Q^2_{\rm RMS}$ measured with uniform weights and $b_c = 0$. To calculate this statistic, we make a weighted least-squares fit of the form

$$t_i^A(\theta, \phi) = \sum_{l=0}^{2} \sum_{m=-l}^{l} a_{lm}^A F_{lm}(\theta, \phi) \qquad (19)$$

to the part of the maps with $|b| > 20°$ and then find

$$Q^2_{\rm RMS} = \sum_{m=-2}^{2} a_{2m}^A a_{2m}^B \,. \qquad (20)$$

This is equivalent to calculating $Q_{\rm RMS}$ for the sum and difference maps and then using $Q^2 = Q^2[(A + B)/2] - Q^2[(A - B)/2]$. With a $|b| > 20°$ cut the value of Q is 10.4 μK (Planck) from the 1 yr 53 GHz maps corrected for the kinematic quadrupole. The value 11 ± 3 μK for this statistic in Smoot et al. (1992) is just the quadrupole of the kinematically corrected sum map. This case is one of the lower values that went into the cosmic quadrupole estimate $Q = 13 \pm 4$ μK in Bennett et al. (1992b), but it is nonetheless a high confidence detection, since it is exceeded by only one out of 4998 Monte Carlo skies[9] with $\langle Q^2_{\rm RMS}\rangle^{0.5} = 0$. Even with this low value, the the large cosmic variance causes Monte Carlo skies with $\langle Q^2_{\rm RMS}\rangle^{0.5} = 16.66$ μK to have actual $Q_{\rm RMS} < 10.4$ μK 13% of the time, as shown in Figure 8.

The column labeled VQ20 in Table 1 gives the m-averaged response of the actual quadrupole statistic to the spherical harmonics F_{lm}. Note the strong response to $l = 4$ caused by the Galactic plane cut. The small responses to odd l's are due to the use of a weighted fit for the quadrupole, since the pattern of the weights has a slight N-S asymmetry.

[9] For $\langle Q^2_{\rm RMS}\rangle^{0.5} = 0$, symmetry can be used to double the effective number of trials.

6. PARAMETER ESTIMATION AND LIKELIHOOD

We have made extensive Monte Carlo calculations that give us the probability of obtaining a given value of $\sigma^2_{\rm sky}(10°)$ or S when the value of the model parameter $\langle Q^2_{\rm RMS}\rangle^{0.5}$ is specified. We can denote the results of the Monte Carlo calculations as $P(D \mid M)$, the probability of a given data value D as a function of the model M. This is the *likelihood* function. But the purpose of the DMR experiment is to determine the value of the parameter $\langle Q^2_{\rm RMS}\rangle^{0.5}$. Bayes's theorem can be used to derive $P(M \mid D)$, the probability of a model given the observed data D:

$$P(M \cap D) = P(M \mid D)P(D) = P(D \mid M)P(M) \,, \qquad (21)$$

where $P(M \cap D)$ is the joint probability of a given model and a given dataset, $P(D)$ is the probability of the data, and $P(M)$ is the *prior* distribution of the model, the source of many disputes between Bayesian and frequentist statisticians. Here we will just assume that $P(M)$ is a constant, which leads to the maximum likelihood method of parameter estimation.

Since both the $\sigma^2_{\rm sky}(10°)$ and the Boughn-Cottingham statistics have $l_{\rm eff} \approx 4$, we cannot estimate both $\langle Q^2_{\rm RMS}\rangle^{0.5}$ and the spectral index n, so we will only estimate the single parameter $\langle Q^2_{\rm RMS}\rangle^{0.5}$ for a fixed $n = 1$. Using the quadratic interpolation technique, we can find the number of Monte Carlo cases that give values within a range $D + \delta D$ centered on the observed value of the statistic as a function of $\langle Q^2_{\rm RMS}\rangle^{0.5}$. We have selected δD so that about 800 of the 2499 Monte Carlo runs for each statistic fall within the range at the peak. The number of Monte Carlo runs within these ranges centered on the observed value is shown in Figure 9 for GET_SKY_RMS in $|b| > 20°$, DMRSMUTH in $|b| > 30°$, and the Boughn-Cottingham statistic $S = |b| > 20°$ with monopole, dipole and quadrupole removed. Also shown as ticks near the peak of each likelihood curve are the values of $\langle Q^2_{\rm RMS}\rangle^{0.5}$ derived by setting the mean of the Monte Carlo runs equal to the

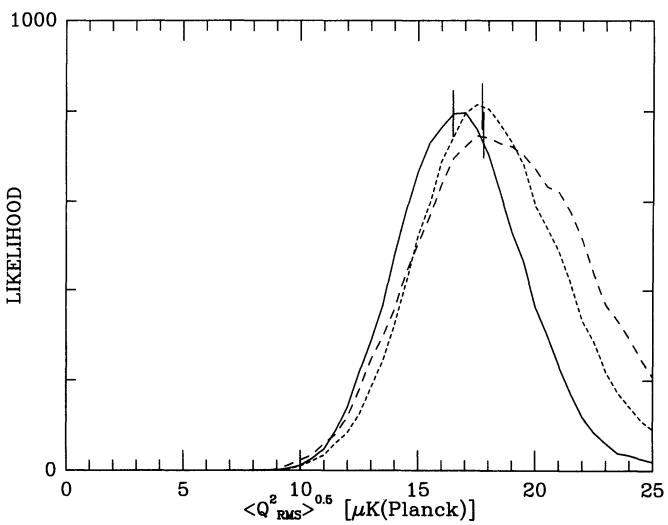

FIG. 9.—The number of Monte Carlo runs within a range centered on the observed value of the statistic for GET_SKY_RMS with $|b| > 20°$ (*solid line*), DMRSMUTH with $|b| > 30°$ (*short dashed line*), and S with $|b| > 20°$ (*long dashed line*). Mean-derived estimates of $\langle Q^2_{\rm RMS}\rangle^{0.5}$ are indicated by vertical lines near the peaks of the likelihood curves.

observed values. These values are close to the maximum likelihood values in all three cases, and are all within the $N^{1/2}$ uncertainty of the peak. Since these mean-derived estimates of $\langle Q_{\rm RMS}^2 \rangle^{0.5}$ are more easily extended to other values of n using equation (11) and the values in Table 1, we are reporting the mean-derived values for $\langle Q_{\rm RMS}^2 \rangle^{0.5}$ below.

7. SUMMARY AND CONCLUSIONS

We have shown that using the actual DMR beam and the actual computer programs for smoothing the DMR maps gives a ratio of excess sky variance to $\langle Q_{\rm RMS}^2 \rangle$ that is from 10% to 20% lower than a simple smoothing with a 10° Gaussian applied to the whole sky. The effect of the Galactic plane cut on the quadrupole and octupole affects all statistical analyses of the DMR data, including analyses of the correlation functions. Any statistic calculated from the DMR maps should be compared to the results from Monte Carlo sky simulations. Smoot et al. (1992) and Wright et al. (1992) both used libraries of expected correlation functions for different values of n that were evaluated using Monte Carlo simulations that included the $|b|$ cut, but used the Gaussian approximation to the DMR beam.

When these precautions are applied to the $\sigma_{\rm sky}(10°)$ statistic we get the following results: with a 20° cut, DMRSMUTH gives $\langle Q_{\rm RMS}^2 \rangle^{0.5} = 18.3$ μK and GET_SKY_RMS gives $\langle Q_{\rm RMS}^2 \rangle^{0.5} = 16.5$ μK when applied to the 53 GHz maps. With a 30° cut, DMRSMUTH gives $\langle Q_{\rm RMS}^2 \rangle^{0.5} = 17.7$ μK and GET_SKY_RMS gives $\langle Q_{\rm RMS}^2 \rangle^{0.5} = 17.0$ μK. The difference between DMRSMUTH and GET_SKY_RMS for $|b| > 30°$ is caused by the interaction between the pattern of the DMR weights and the pattern of the actual variation on the sky. The variance of the DMRSMUTH maps computed using weights gives a $\langle Q_{\rm RMS}^2 \rangle^{0.5}$ that is 4%–5% smaller than that calculated without weights. While using weights reduces the effect of radiometer noise, it increases the effect of cosmic variance. For the $|b| > 20°$ cut, DMRSMUTH actually uses data within 9°.5 of the Galactic plane and as a result is picking up some Galactic signal. Thus neither GET_SKY_RMS nor DMRSMUTH can be considered the "best" way to compute $\sigma_{\rm sky}(10°)$, and we have averaged together the values for $\langle Q_{\rm RMS}^2 \rangle^{0.5}$ given above without including DMRSMUTH at $|b| > 20°$. This gives $\langle Q_{\rm RMS}^2 \rangle^{0.5} = 17.1 \pm 2.9$ μK for $n = 1$ where the error is purely statistical. While Galactic emission should have only a small effect on $\sigma_{\rm sky}(10°)$ and S, based on Figure 4 of Bennett et al. (1992b), we caution that no allowance has been made for the systematic error limits discussed in Kogut et al. (1992). The actual quadrupole in the DMR maps is considerably smaller than this value of $\langle Q_{\rm RMS}^2 \rangle^{0.5}$. As a result, the Boughn-Cottingham statistic S which is based solely on $l > 2$ gives a slightly higher value $\langle Q_{\rm RMS}^2 \rangle^{0.5} = 17.8 \pm 3.8$ μK, where the error is again purely statistical. Thus both the $\sigma_{\rm sky}(10°)$ and Boughn-Cottingham statistic of the DMR maps are consistent with the $\langle Q_{\rm RMS}^2 \rangle^{0.5} = 17 \pm 5$ μK reported by Smoot et al. (1992) and Wright et al. (1992), but the statistical error on $\langle Q_{\rm RMS}^2 \rangle^{0.5}$ is only 3 μK. Since both $\sigma_{\rm sky}(10°)$ and S have $l_{\rm eff} \simeq 4$, a less n-dependent statement of the results of this paper is that power-law power spectra that match the amplitude of the structure seen in the DMR maps have an rms hexadecupole of $\langle \Delta T_4^2 \rangle^{0.5} = (12.8 \pm 2.3)$ μK, where we have now included (in quadrature) the estimated systematic error in the hexadecupole from Kogut et al. (1992).

We particularly thank the computer scientists and technical staff at Goddard Space Flight Center, who wrote and debugged many complex programs to sort, analyze, and calibrate the DMR data. The high quality of the data set is the result of many thousands of hours of detailed inspection of the data and checking of the software. In particular, we thank A. Banday, P. Jackson, E. Kaita, P. Keegstra, V. Kumar, R. Kummerer, K. Lowenstein, and J. Santana.

REFERENCES

Adams, F. C., Bond, J. R., Freese, K., Frieman, J. A., & Olinto, A. V. 1993, Phys. Rev. D, 47, 426
Bennett, C. L., et al. 1992a, ApJ, 391, 466
Bennett, C. L., et al. 1992b, ApJ, 396, L7
Bond, J. R., & Efstathiou, G. 1987, MNRAS, 226, 655
Boughn, S. P., Cheng, E. S., Cottingham, D. A., & Fixsen, D. J. 1992, ApJ, 391, L49
Fixsen, D. J., et al. 1994, ApJ, in press
Kogut, A., et al. 1992, ApJ, 401, 1
Kogut, A., et al. 1993, ApJ, 419, 1
Smoot, G. F., et al. 1991, ApJ, 371, L1
Smoot, G., et al. 1992, ApJ, 396, L1
Toral, M. A., Ratliff, R. B., Lecha, M. C., Maruschak, J. G., Bennett, C. L., & Smoot, G. F. 1989, IEEE Trans. Ant. Prop., 37, 171
Wright, E. L. 1991, Results from *COBE*, talk at the Caltech Centennial Symposium, September 26
———. 1993, in 16th Texas Symp. in Relativistic Astrophysics, Ann. NY Acad. Sci., 698, 836
Wright, E. L., et al. 1992, ApJ, 396, L13